Calibration of the Underwater Coordinate Measuring Machine Using Multi-joint Link

Soji Shimono, Uichi Nishizawa, and Shigeki Toyama

***Abstract*—In this paper, the calibration of the multi-joint serial link for underwater coordinate measuring machine is conducted. The underwater coordinate measuring machine is an underwater positioning system which consists of underwater robot and multi-joint link. The link connected underwater robot from the water surface. The position of the robot is obtained from kinematics of the multi-joint link. The geometric calibration of the experimental model of the multi-joint link is conducted at the water tank and atmosphere to evaluate its measurement accuracy. The calibration result indicate that the positioning accuracy of the experimental model at the underwater is better than atmosphere and its standard deviation is 0.59 mm is obtained.**

***Index Terms*—Underwater positioning, multi joint serial link, calibration.**

I. Introduction

This paper reports the result of calibration about underwater coordinate measuring machine (UWCMM) which is proposed for underwater positioning. The UWCMM consist of underwater robot and multi-joint serial link (Fig. 1). The position information is necessary for underwater works. But the global navigation satellite system is not available at the underwater. Thus, generally, the acoustic positioning system or inertial navigation system are used [1], [2]. The UWCMM is alternative method for underwater positioning. The position of the underwater robot that equipped at the tip of the multi-joint link is obtained from the kinematics of the multi-joint link. This method can stable measurement near the complicated structure that occur positioning error to the acoustic positioning system due to the multi pass of the sound wave. And the position drift that appear inertial positioning system is not occur in this method. Authors have developed the experimental model of the UWCMM for evaluation of this positioning method. This paper report calibration of the multi-joint link conducted to evaluate the measurement accuracy of the experimental model.

The position of the tip of the multi-joint link is calculated from joint angle and geometric parameter of the link. However these parameter include machining error and assemble error, so these produce positioning error. Furthermore, non-geometric parameter such as deflection of the link and backlash of the joint also produce positioning error. Because these parameters are necessary to Calibrate for accurate positioning. The calibration of the multi-joint link is studied for industrial manipulator. The category of the calibration method is able to divide Level I, Level II and Level III [3], [4]. The Level I calibration reduce joint angle offset error that has large effect. Level II calibrate not only joint angle offset but also geometric error such as link length error due to the machining or assemble. In addition to the geometric parameter, Level III calibration compensate non-geometric error such as deflection and backlash. Kinematics model of level III calibration also include such non-geometric factor. And the other calibration method using neural net is also studied [5], [6]. In this paper, as the first step, level I and level II calibration is conducted to the experimental model of multi-joint serial link for UWCMM in order to evaluate its accuracy. The calibration is implemented using dataset that consist of some known positon of the measurement points and Joint angle while measuring these point. The UWCMM is used in the underwater thus the dataset is obtained in the water tank and the calibration is implemented using this data set. In this paper, used calibration method and the experimental model are explained. Then calibration experiment and its result are reported.

Manuscript received May 20, 2018; revised June 12, 2018.

Soji Shimono is with the Q.I Incorporated, 4-7, Fukuura 2-chome, kanazawa-ku, Yokohama, Japan. And also with the Tokyo University of Agriculture and Technology, Japan (e-mail: shimono@qi-inc.com).

U. Nishizawa and S. Toyama are with the Tokyo University of Agriculture and Technology, 2-24-16, Nakacho, Koganei, Tokyo, Japan (e-mail: n-uichi@cc.tuat.ac.jp, toyama@cc.tuat.ac.jp).

II. Experimental Model

The appearance of the experimental model is shown in Fig. 2. To implement calibration, a steel ball is attached to the tip of the serial link as the probe, and the serial link is set to an aluminum flame. The weight in air of experimental model is 2.9 kg, and weight in water is approximately 1kg. The total length is 1.9 m.

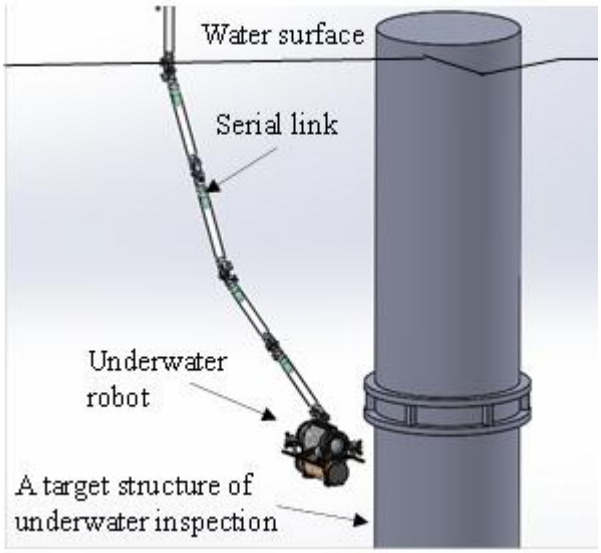

Fig. 1. Conceptual diagram of the UWCMM.

DOI: 10.7763/IJMO.2018.V8.654

The number of joints of the serial link is five, and each joints and links are of the same design. One joint has single axis, which is twisted by 90 ° from the next joint in the axial direction of the link. The DH parameters of the serial link are shown in Table I. Each axis has an absolute rotary encoder, which has 18-bit resolution. The joint also has geared motor. But it is not used for this experiment. The joints are connected with flanged acrylic pipe. The axis and the connection between the joint and link are sealed with an O-ring to keep the inside of the link dry and at atmospheric pressure. The microcontroller is included in the link pipe and transmits the joint angle data measured by the encoder through the CAN communication. All links have same design and so the number of joint can be easily reconfigured by the addition or removal of a link module.

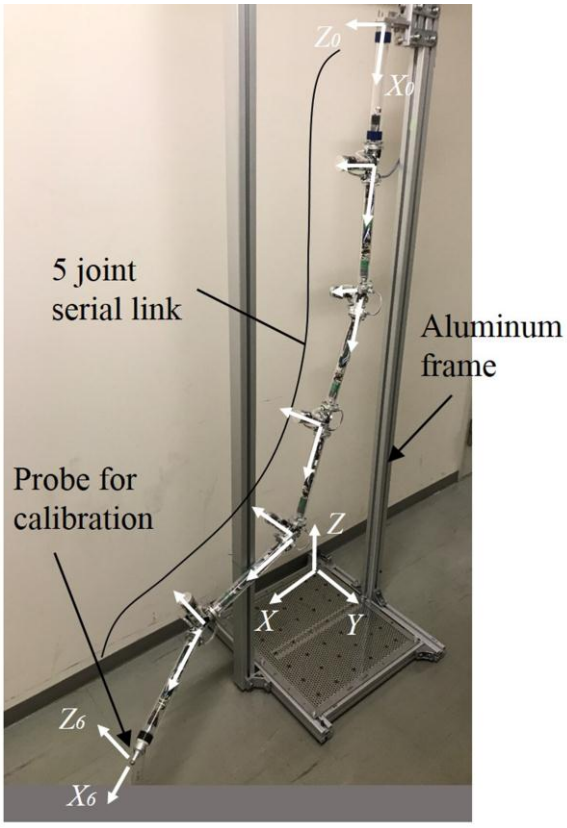

Fig. 2. Appearance of experimental model

TABLE I: DH PARAMETER OF THE EXPERIMENTAL MODEL

Joint	a (mm)	d (mm)	α (degree)	θ (degree)
0- > 1	284	0	0	θ1
1 -> 2	330	0	90	θ2
2 -> 3	330	0	-90	θ3
3 -> 4	330	0	90	θ4
4 -> 5	330	0	-90	θ5
5 -> 6	339	-	-	-

III. CALIBRATION METHOD

The calibration of the experimental model is implemented to evaluate the accuracy. The position of the probe which attached on the tip is calculated with the joint angle measured by the encoder and the geometric parameter of the serial link. However, these parameters have some machining error and assembly error, against design value. Thus it is necessary to calibrate against these errors to properly position the probe. Therefore, geometric calibration was implemented using pseudo inverse matrix. The method is shown below.

The position vector $\boldsymbol{r}$ of probe is the function of the joint angles $\boldsymbol{q}$ and link parameter $\boldsymbol{\varphi}$. Then change of $\boldsymbol{r}$ against small displacement $\Delta\boldsymbol{\varphi}$ is expressed by equation (2).

$$\boldsymbol{r} = (x(\boldsymbol{q}, \boldsymbol{\varphi})\ \ y(\boldsymbol{q}, \boldsymbol{\varphi})\ \ z(\boldsymbol{q}, \boldsymbol{\varphi}))^T \tag{1}$$

$$\begin{pmatrix}\Delta x\\ \Delta y\\ \Delta z\end{pmatrix} = \begin{pmatrix} \frac{\partial x}{\partial a_1} & \frac{\partial x}{\partial d_1} & \cdots & \frac{\partial x}{\partial \alpha_5} & \frac{\partial x}{\partial \theta_{d5}} \\ \frac{\partial y}{\partial a_1} & \frac{\partial y}{\partial d_1} & \cdots & \frac{\partial x}{\partial \alpha_5} & \frac{\partial x}{\partial \theta_{d5}} \\ \frac{\partial z}{\partial a_1} & \frac{\partial z}{\partial d_1} & \cdots & \frac{\partial x}{\partial a_5} & \frac{\partial x}{\partial \theta_{d5}} \end{pmatrix} \Delta\boldsymbol{\varphi} \tag{2}$$

$$\boldsymbol{q} = (\theta_{q1}\ \ \theta_{q2}\ \ \theta_{q3}\ \ \theta_{q4}\ \ \theta_{q5}) \tag{3}$$

$$\boldsymbol{\varphi} = (a_1\ \ d_1\ \ \alpha_1\ \ \theta_{d1}\ \cdots\ a_5\ \ d_5\ \ \alpha_5\ \ \theta_{d5}) \tag{4}$$

θ_q are measured value of each joints encoder and their offset angle is defined as θ_d that will be calibrated. Joint angle $\theta = \theta_q + \theta_d$.

$\Delta\boldsymbol{x}$, $\Delta\boldsymbol{y}$, $\Delta\boldsymbol{z}$ are defined as the difference between actual position of the probe and calculated position obtained from equation (1). When n of measuring point are obtained, the relationship between position difference and small displacement of parameter $\boldsymbol{\varphi}$ is shown below.

$$\begin{pmatrix}\Delta\boldsymbol{r}_1\\ \Delta\boldsymbol{r}_2\\ \vdots\\ \Delta\boldsymbol{r}_n\end{pmatrix} = \begin{pmatrix}\frac{\partial \boldsymbol{r}_1}{\partial\boldsymbol{\varphi}} & \frac{\partial \boldsymbol{r}_2}{\partial\boldsymbol{\varphi}} & \cdots & \frac{\partial \boldsymbol{r}_n}{\partial\boldsymbol{\varphi}}\end{pmatrix}^T \Delta\boldsymbol{\varphi} \tag{5}$$

Here, $\Delta r = (\Delta x\ \ \Delta y\ \ \Delta z)^T$ and $\partial\boldsymbol{r} / \partial\boldsymbol{\varphi}$ correspond the matrix which product to the $\Delta\boldsymbol{\varphi}$ in the equation (2). The correction value of the $\boldsymbol{\varphi}$ is obtained from equation (6). $\boldsymbol{J^{-1}}$ is the pseudo inverse matrix of right side matrix that product $\Delta\boldsymbol{\varphi}$ in the equation (5). The parameter $\boldsymbol{\varphi}$ can calibrate using $\Delta\boldsymbol{\varphi}$. This procedure is repeated while $\boldsymbol{\varphi}$ will be convergence.

$$\Delta\boldsymbol{\varphi} = J^{-1} (\Delta\boldsymbol{r}1\ \ \Delta\boldsymbol{r}2\ \cdots\ \Delta\boldsymbol{r}n)^T \tag{6}$$

$$\boldsymbol{\varphi}_i = \boldsymbol{\varphi}_{i-1} + \Delta\boldsymbol{\varphi} \tag{7}$$

IV. EXPERIMENT

A measurement experiment was conducted to obtain a dataset that consists of the probe position and the joint angle for calibration purposes. The probe is set at the measurement point and has a known position and the joint angle was obtained from the encoder and was recorded through the CAN communication. Measurement points were 42 holes placed on the punched stainless board which were fixed to the aluminum frame. The board is shown in Fig. 3. The probe is placed on these measurement holes and its position can then be set to a known position. The probe is manually manipulated. The position between root link of the experimental model and the origin of the stainless board was manually measured. The measurement was conducted at a water tank and at the atmosphere. To obtain a variety of postures of the serial link, the direction of the tip was set to two patterns: oriented to the origin of the board and in the opposite direction. The former is defined as posture A, and

the latter is defined as posture B (Fig. 4). Measuring the 42 points on the board is defined as one set, three sets of measurements are obtained from posture A and B respectively. In total, 252 points of the dataset were obtained from the experiment. After the underwater measurement, a very little of water was flooded into the second link from the tip and the backlash of the first joint was slightly increased.

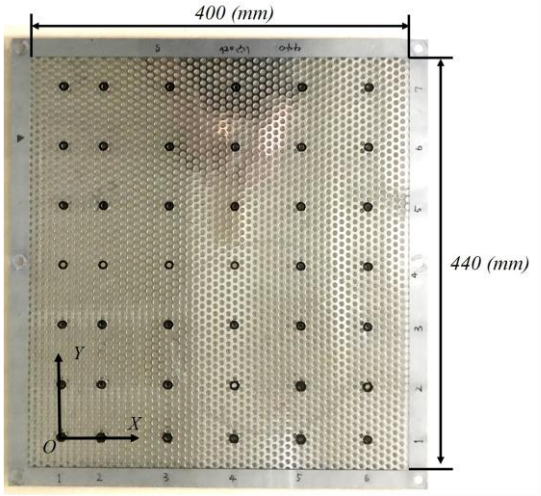

Fig. 3. Measured hole on the board.

Posture A Posture B

Fig. 4. Posture A and B.

V. Result

For verification, 42 points of the dataset of one cycle for posture A were used, and the other dataset was used for calibration. Two types of calibration were implemented. One was to calibrate only the angular parameters of the serial link and the other was to calibrate all the parameters. Here, the former was denoted as calibration I, and the latter denoted as calibration II.

A. Calibration result of Underwater Measurement

The probe position on the *x-y* plane obtained from kinematics before calibration using calibration data set is shown Fig. 5. And the result of calibration I is shown in Fig. 6. The Black marks shows the position of the measured holes. The probe position error of the verification data set using the parameters obtained by calibration I is shown Fig. 7. The position error is defined as the difference from the hole position. The result of calibration II is also shown in Figs. 8 and 9. The correction value of the DH parameters of calibration I and II are shown Table II, and III, respectively. The standard deviation and maximum value of the 3D-positional error of the probe were obtained from the verification data set, and are summarized in Table V. Fig. 5, 6 and 8 indicate that both calibration methods reduced the position error of the probe. The maximum position error and the standard deviation of calibration II is smaller than I, but the length of the process parameters are incorrect, they vary hugely from the design value.

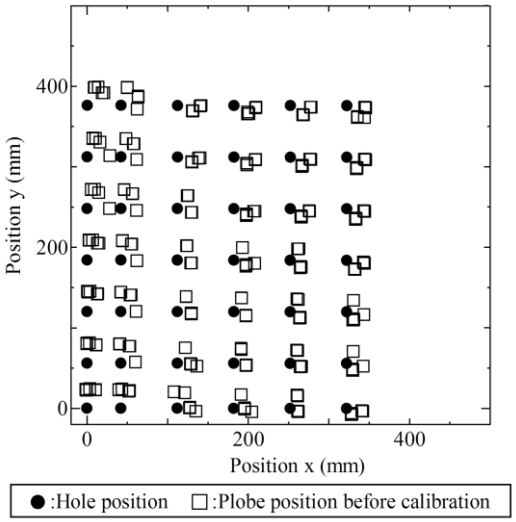

Fig. 5. Horizontal hole position of calibration data set at the underwater before calibration.

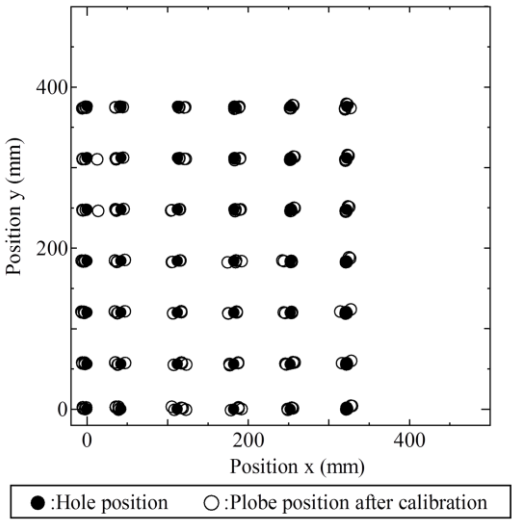

Fig. 6. Horizontal hole position of calibration data set at underwater after calibration I.

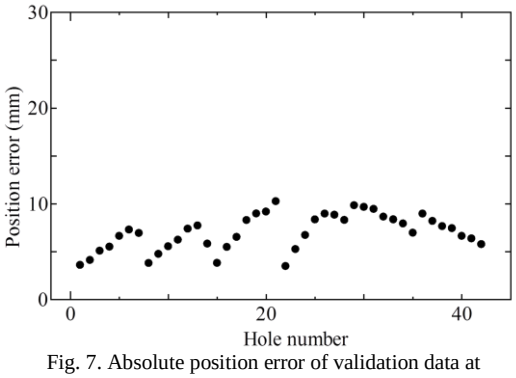

Fig. 7. Absolute position error of validation data at underwater after calibration I.

TABLE II: Correction Value of The DH Parameter Obtained from Calibration I at Underwater

Joint	a (mm)	d (mm)	α (degree)	θ (degree)
0- > 1	0.00	0.00	-1.41	-1.12
1 -> 2	0.00	0.00	-0.02	-0.70

2 -> 3	0.00	0.00	-0.25	1.40
3 -> 4	0.00	0.00	-1.32	-0.15
4 -> 5	0.00	0.00	1.21	0.27
5 -> 6	0.00	-	-	-

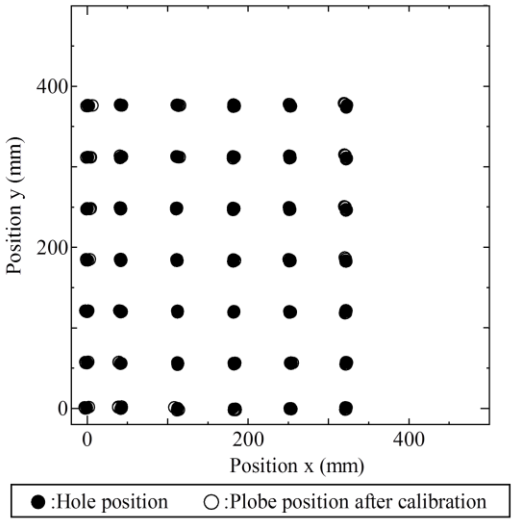

Fig. 8. Horizontal hole position of calibration data set at underwater after calibration II.

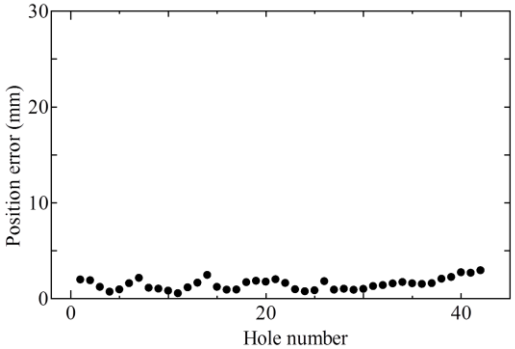

Fig. 9. Absolute position error of validation data at underwater after calibration II.

TABLE III: CORRECTION VALUE OF THE DH PARAMETER OBTAINED FROM CALIBRATION II AT UNDERWATER

Joint	a (mm)	d (mm)	α (degree)	θ (degree)
0- > 1	0.79	-4.55	-1.19	-0.78
1 -> 2	-17.66	-1.39	-0.14	-0.24
2 -> 3	14.97	-3.50	0.28	0.84
3 -> 4	5.52	3.41	-1.88	-1.03
4 -> 5	0.97	6.06	0.81	0.52
5 -> 6	0.71	-	-	-

B. Calibration Result of Measurement at the Atmosphere

The data set obtained at the atmosphere was also processed. The probe position on the x-y plane obtained from kinematics before calibration using calibration data set is shown Fig. 10. And the result of calibration I is shown in Fig. 11. The parameters are divergence at the calibration II. The probe position error calculated from the verification data set after calibration is shown in Fig. 12. The positional error of the probe was seen to decrease. The maximum error and standard deviation of the verification data set is also shown in Table. V. It is larger than the dataset measured underwater. The correction value of the DH parameter after calibration is shown in Table IV.

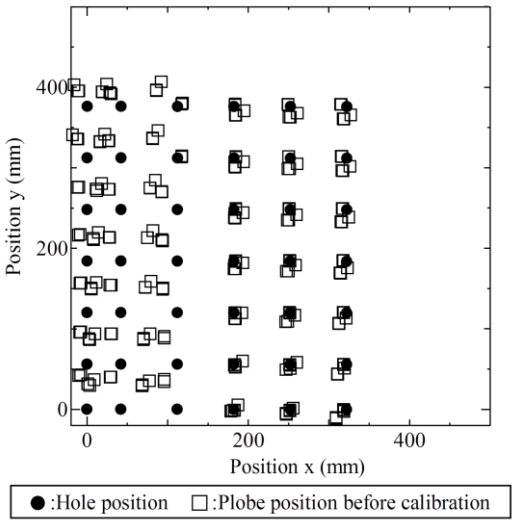

Fig. 10. Horizontal hole position of calibration data set at the atmosphere before calibration

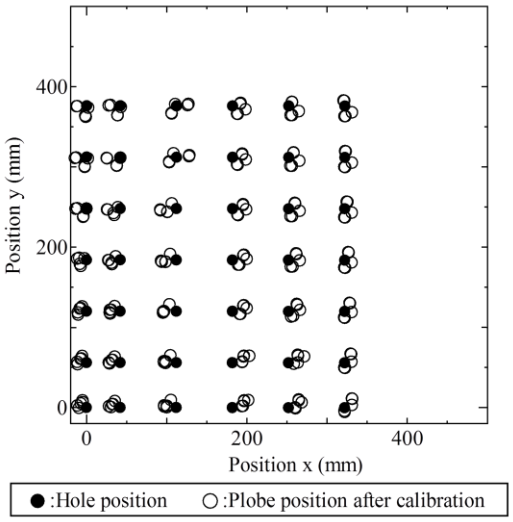

Fig. 11. Horizontal hole position of calibration data set at atmosphere after calibration I.

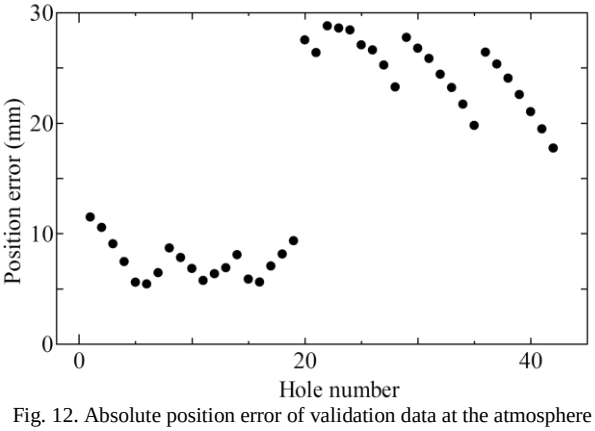

Fig. 12. Absolute position error of validation data at the atmosphere after calibration I.

TABLE IV: CORRECTION VALUE OF THE DH PARAMETER OBTAINED FROM CALIBRATION I AT ATMOSPHERE

Joint	a (mm)	d (mm)	α (degree)	θ (degree)
0- > 1	0.00	0.00	-0.72	-1.55
1 -> 2	0.00	0.00	-0.02	-0.27
2 -> 3	0.00	0.00	-0.85	2.39
3 -> 4	0.00	0.00	-1.42	2.13
4 -> 5	0.00	0.00	1.89	-1.16
5 -> 6	0.00	-	-	-

TABLE V: MAXIMUM ERROR AND STANDARD DEVIATION

	σ	Maximum error (mm)
Calibration I (underwater)	1.83	10.26
Calibration II (underwater)	0.59	2.95
Calibration I (atmosphere)	8.23	28.8

VI. DISCUSSION

The positional error of the probe obtained by calibration II was smaller than that from calibration I at the underwater measurement. This can be explained as the positional error, which cannot correct only the angular calibration, was treated by a range of lengths of the parameter. The range of the length parameters is larger than the error assumed during machining. It can be assumed that the measurement area is limited and the calibrated parameters are optimized to the conditions. Alternatively, the non-geometric parameters such as deflection of the joint produce positional errors affect the calibrated geometric parameters.

Underwater measurements had a smaller positional error of the probe than the measurements at the atmosphere. Some factors that affected the measuring accuracy of UWCMM, i.e., buoyancy, water pressure, and water current were not considered. The buoyancy is the main factor in this experiment. The experiment was conducted at a closed pool depth of approximately 2 m. Thus, there was no water current and displacement of the serial link due to water pressure was negligible. It is considered that the buoyancy reduces the weight of the serial link in the water and the joint bending that produces non-geometric errors. To obtain a higher accuracy, joint bending will become a problem in underwater measurements. A possible solution is to consider a model that includes non-geometric factors and its calibration method, or by increasing the joint stiffness. However, the latter is not practical because high stiffness makes the arm larger. Such a serial link becomes heavy and creates too much drag on the water. Hence a large serial link is difficult to deploy in reality.

VII. SUMMARY AND FUTURE WORKS

In this study, the calibration of the experimental model of multi-joint link for UWCMM, which consists of a serial link and ROV, was conducted to evaluate the position calculation accuracy. The used calibration method for geometric error was explained and the calibration was conducted in the water and atmosphere. Maximum error was noted as 2.95 mm and 28.8 mm in water and atmospheric conditions, respectively. Underwater measurements were highly accurate. It seems that buoyancy affected the serial link and reduced non-geometric error produced by the weight of the serial link.

In future works, other calibration methods using a neural net to increase accuracy will be considered. And the evaluation of the effect of the water current on the accuracy also will be considered.

REFERENCES

[1] P. Y. Tao and G. Yang, "Calibration of industrial robots with product-of-exponential (POE) model and adaptive neural networks," in Proc. *2015 IEEE International Conference, Seattle Robotics and Automation (ICRA)*, WA, 26-30 May 2015

[2] J. H. Jang, S. H. Kim, and Y. K. Kwak, "Calibration of geometric and non-geometric errors of an industrial robot," *Robotica*, vol.19, no. 3, pp. 311-321, May. 2001.

[3] H. P. Tan, R. Diamant, W. K. G. Seah, and M. Waldmeyer, "A survey of techniques and challenges in underwater localization," *Ocean Engineering*, vol 38, no. 14-15, pp. 1663-1676, October 2011

[4] B. Mooring, M. Driels, and Z. Roth, *Fundamentals of Manipulator Calibration*, J. Wiley, 1991

[5] A. Y. Elatta, L. P. Gen, F. L. Zhi, Y. Daoyuan, and L. Fei, "An overview of robot calibration," *Information Technology Journal*, vol. 3, no. 1, pp. 74-78, January 2004

[6] P. Y. Tao and G. Yang, "Calibration of industrial robots with product-of-exponential (POE) model and adaptive neural networks," in *Proc. 2015 IEEE International Conference on Robotics and Automation (ICRA)*, Seattle, WA, 26-30 May 2015

[7] J. H. Jang, S. H. Kim, and Y. K. Kwak, "Calibration of geometric and non-geometric errors of an industrial robot," *Robotica*, vol. 19, no.3, pp.311-321, May 2001.

Soji Shimono was born in Tokyo, Japan, in 1988. He received his B.E., M.E., in mechanical engineering from Tokai University, Japan in 2009, 2011, respectively. He is 4th year student in the doctoral program of Tokyo University of Agriculture and Technology. Since 2012, He is an engineer of Q.I incorporated. His primary research interests include robotics. He is a member of the Marine Technology Society.

Uichi Nishizawa received the Ph.D. degree in engineering from Tokyo University of Agriculture and Technology, Tokyo, Japan, in 2008. Now he works at Tokyo University of Agriculture and Technology. His current research interests include robotics, aerospace engineering, and welfare technology.

Shigeki Toyama received Ph.D. degree in engineering from University of Tokyo, Tokyo, Japan, in 1981. Now he works at Tokyo University of Agriculture and Technology. His current research interests include robotics, actuator, and welfare technology.